SRR-91-05

Evaluation by Testing of a Bridge with Girders, Floor Beams and Stringers

Ontario

Ministry of Transportation

Research and Development Branch

Ontario
Ministry of Transportation
Research and Development Branch

Documentation Page

SRR-91-05

Evaluation by Testing of a Bridge with Girders, Floor Beams and Stringers

Author(s): B. Bakht - Research and Development Branch
A. Mufti - The Technical University of Nova Scotia

Date Published: September, 1992

Published by: Research and Development Branch, MTO

Contact Person: Baidar Bakht, Structures Research Office
(416) 235- 4674

Abstract: The Adair bridge is a single span, single lane structure with a clear span of 12.8 m. It comprises a non-composite deck slab supported by two outer steel girders and five inner steel stringers with the latter spanning between the abutments but also supported within the span by two transverse floor beams that frame into the girders. This report describes the evaluation by testing of the Adair bridge. This bridge was posted for 6 tonnes before the test. After the test, the load restriction was recommended to be raised to either a single posting of 12 tonnes or a multiple posting of 12, 19, and 26 tonnes.

The pretest evaluation found the girders to be the weakest component of the bridge having a scale down factor of about 0.37. The scale-down factors for the floor beams and stringers were found to be 0.84 and 0.58, respectively. On the basis of the test results, the scale-down factors for the girders, floor beams and stringers were found to be 0.67, 0.62, and 0.62, respectively.

Despite the absence of mechanical shear connectors, the stringers acted compositely with the concrete deck slab. The girders, however, were found to be acting non-compositely. Substanital bearing restraint was observed at the girder supports. This restraint did not enhance the load carrying of the girders which was governed by stresses in their top flanges.

Comments:

Key Words: Adair bridge, evaluation, slab-on-girder bridge, testing

Copyright Status: Crown copyright © 1992 Ministry of Transportation

93-00167/ SRR-91-05

Evaluation by Testing of a Bridge with Girders, Floor Beams and Stringers

B. Bakht
Principal Research Engineer
Research and Development Branch

A. Mufti
Professor of Civil Engineering and
Director of NS CAD/CAM Centre
The Technical University of Nova Scotia

Published by
The Research and Development Branch
Ontario Ministry of Transportation

Published without prejudice as to the application of the findings.
Crown copyright reserved; however, this document may be reproduced for non-commercial purposes with attribution to the Ministry.

For additional copies, contact:
The Editor, Technical Publications
Room 320, Central Building
1201 Wilson Avenue
Downsview, Ontario
Canada M3M 1J8

Telephone: (416) 235-3480
Fax: (416) 235-4872

September 1992

Table of Contents

1/ Test Summary 1

2/ Bridge Description 2

3/ Reasons for Testing 4

4/ Dead Load Analysis 5

4.1/ Usual Practice 5

4.2/ Rigorous Analysis 7

5/ Instrumentation and Testing 9

5.1/ Instrumentation 9

5.1.1/ Girders 9

5.1.2/ Floor Beams 9

5.1.3/ Stringers 9

5.2/ Loads 11

6/ Recorded Data and Its Interpretation 15

6.1/ Girders 15

6.1.1/ Symmetry of Data 18

6.1.2/ Linearity 18

6.1.3/ Bearing Restraint 20

6.1.4/ Calculated Strains 21

6.1.5/ Interpretation of Measured Strains 21

6.2/ Floor Beams 22

6.2.1/ End Restraint 25

6.2.2/ Linearity 25

6.2.3/ Differences Between Top and Bottom Strains 26

6.2.4/ Maximum Strains 26

6.3/ Stringers 27

7/ Strength Evaluation 32

7.1/ Proof Loads 32

7.2/ Equivalent Loads 32

7.3/ Scale-down Factors 32

7.4/ Posting Loads 35

8/ Recommendation 35

References 35

1/ Test Summary

Bridge	:	Adair Bridge, Concession VI, Lot 3,4 Township of Sheffield, County of Lennox-Addington. MTO Site No. 17-20
Type of bridge	:	Concrete slab supported on a frame-work of steel girders, floor beams and stringers.
Posting	:	6 tonnes
Span/width	:	13.26 m / 4.88 m
Angle of skew	:	0°
Date of test	:	May 24, 1990
Test engineer	:	Baidar Bakht
Job captain	:	Jiri Klubal
Supervisor, Instrumentation	:	Bill Kwok
Maximum static load	:	557 kN
Responses measured	:	Strains of girders, floor beams and stringers and vertical deflections of girders.
Recommendations	:	Upgrade posting to either a single posting of 12 tonnes, or a triple posting of 12, 19 and 26 tonnes.

2/ Bridge Description

The Adair bridge (MTO site No. 17-20), located in the Township of Sheffield, County of Lennox-Addington, is a single span, single lane bridge; it comprises a 150 mm thick reinforced concrete deck slab supported on two outer steel girders and five inner steel stringers, with the latter supported in turn by two transverse floor beams that frame into the two girders. All the girders, floor beams and stringers are of rolled steel with sections in the imperial units being 24I100, 18I60 and 9I21, respectively. The properties of these sections are given in Table 2.1, as they are not generally available.

Table 2.1/ Properties of steel sections used in the bridge

component	designation (imperial units)	depth, mm	width, mm	area, mm^2	moment of inertia, mm^4
stringer	9 I @ 21	229	133	3981	36.5×10^6
floor beam	18 I @ 60	464	192	11,380	409.6×10^6
girder	24 I @ 100	610	305	18,968	1240.8×10^6

As shown in Fig. 2.1, the girders are each 13.71 m long with a clear span of 12.80 m. The floor beams located at third points of the girder length, have a spacing of 4.57 m. Also as shown in Fig. 2.1, the centre-to-centre spacing of the longitudinal beams is 0.76 m. Other relevant dimensions of the bridge can be seen in Fig. 2.1.

The date of construction of the bridge is not available; however, some records indicate that the bridge might have been built in the late 1920's.

While the superstructure is in reasonably good condition, each of the abutments has a vertical crack, about 50 mm wide. One such crack can be seen in Fig. 2.2, which also shows a part of the underside of the superstructure.

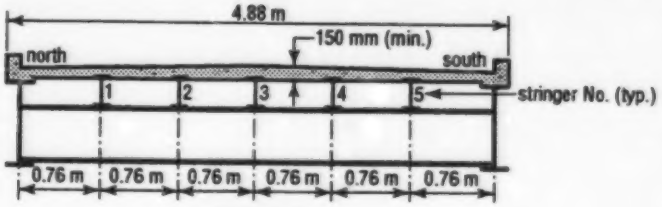

cross-section

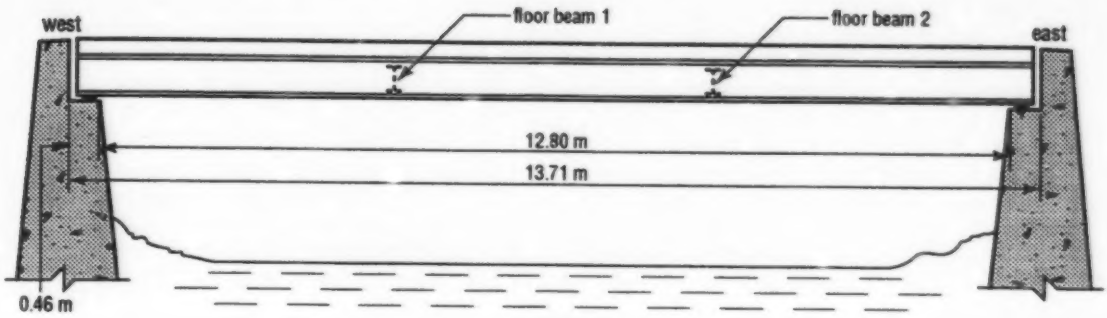

elevation

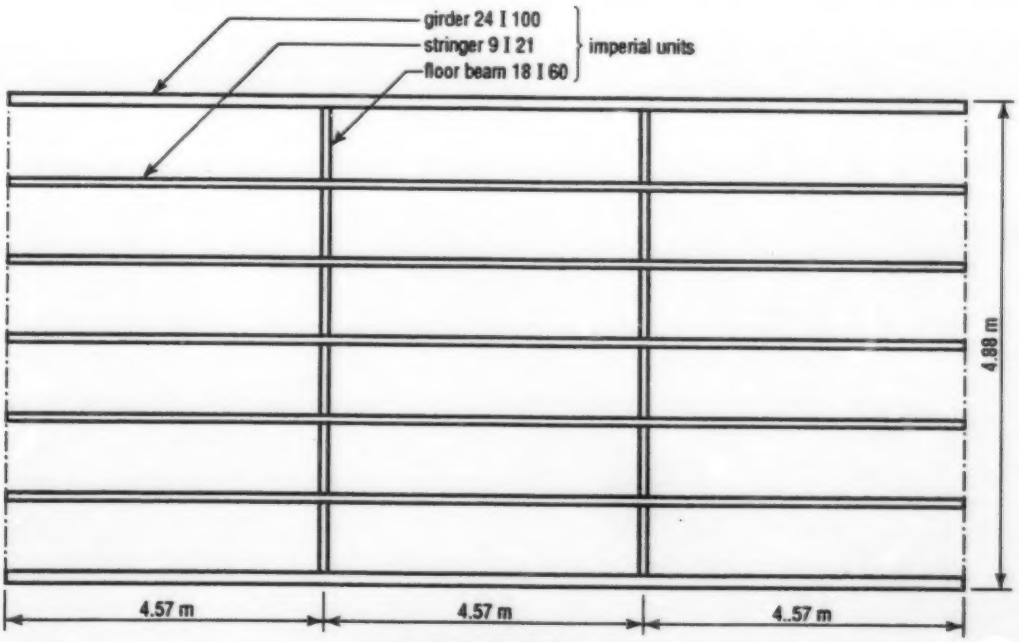

plan of steel beams

Figure 2.1/ Details of the bridge

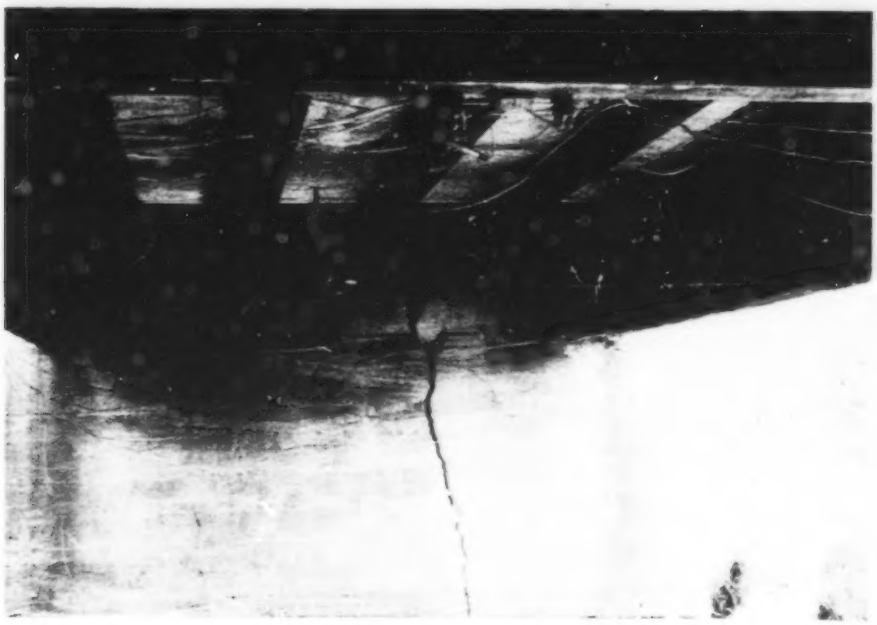

Figure 2.2/ Photograph showing a wide vertical crack in the abutment

3/ Reasons For Testing

Until an analytical evaluation was carried out in 1989, the bridge had been posted in recent years for 15 tonnes. The analytical evaluation showed that the posting of 15 tonnes was excessive, and that the bridge should have either a single posting of 6 tonnes or a triple posting of 6, 7 and 16 tonnes. Following the evaluation, the bridge was posted for 6 tonnes.

The analytical evaluation found the girders to be the weakest link in the bridge; for these components, the scale-down factor, F, (OHBDC, 1983) was found to be about 0.37. The next weakest components were the stringers for which F was found to be about 0.58. The floor beams were the strongest of the steel sections, having F = 0.84.

Since the posting of 6 tonnes represented a significant restriction to the road network of the township, a bridge test was requested in the hope that through evaluation by testing, the posting limit on the bridge can be upgraded to an acceptable limit.

4/ Dead Load Analysis

4.1/ Usual Practice

For the analysis of load effects due to dead loads in the kind of bridge under consideration, it is usual to consider its various components in isolation. For example, as shown in Fig. 4.1 (a), the load effects in the stringers are calculated by assuming that the floor beams provide rigid restraint against vertical deflections. The stringer reactions thus obtained are used as loads on the floor beams, as shown in Fig. 4.1 (b). The analysis of girders is illustrated in Fig. 4.1 (c), in which it can be seen that the floor beam reactions are treated as the loads transferred to the girders from the whole flooring system.

If the stringers are discontinuous over the floor beams, as they sometimes are, the usual approach described above gives fairly accurate results. However, this approach gives somewhat misleading results when the stringers are continuous as they are in the Adair bridge. The errors involved in this case are discussed in the following sub-section.

Following OHBDC (1983), the dead load factors for the deck slab concrete and structural steel were taken as 1.2 and 1.1, respectively. Using these factors, the maximum stresses due to factored dead loads obtained by the usual approach, are listed in Table 4.1.

Table 4.1/ Calculated dead load stresses, and stresses and strains available for factored live loads

component	calculations by usual method			grillage analogy method		
	dead load stress, MPa	available stress for factored L.L., MPa	available strain for factored L.L., mm x 10^6/mm	dead load stress, MPa	available stress for factored L.L., MPa	available strain for factored L.L., mm x 10^6/mm
stringers	17	182	889	43	156	754
floor beams	27	172	831	23	176	851
girders	69	130	628	63	136	657

As specified in the OHBDC (1983), the performance factor for steel is taken as 0.95, and the specified minimum yield stress of the structural steel used in the bridge as 210 MPa; this gives the factored yield stress of 199 MPa. By deducting from the factored yield stress the stresses due to factored dead loads calculated earlier, one obtains the stresses that are available for factored live loads. These available stress levels and corresponding strains, which should not be exceeded during the load test, are also given in Table 4.1.

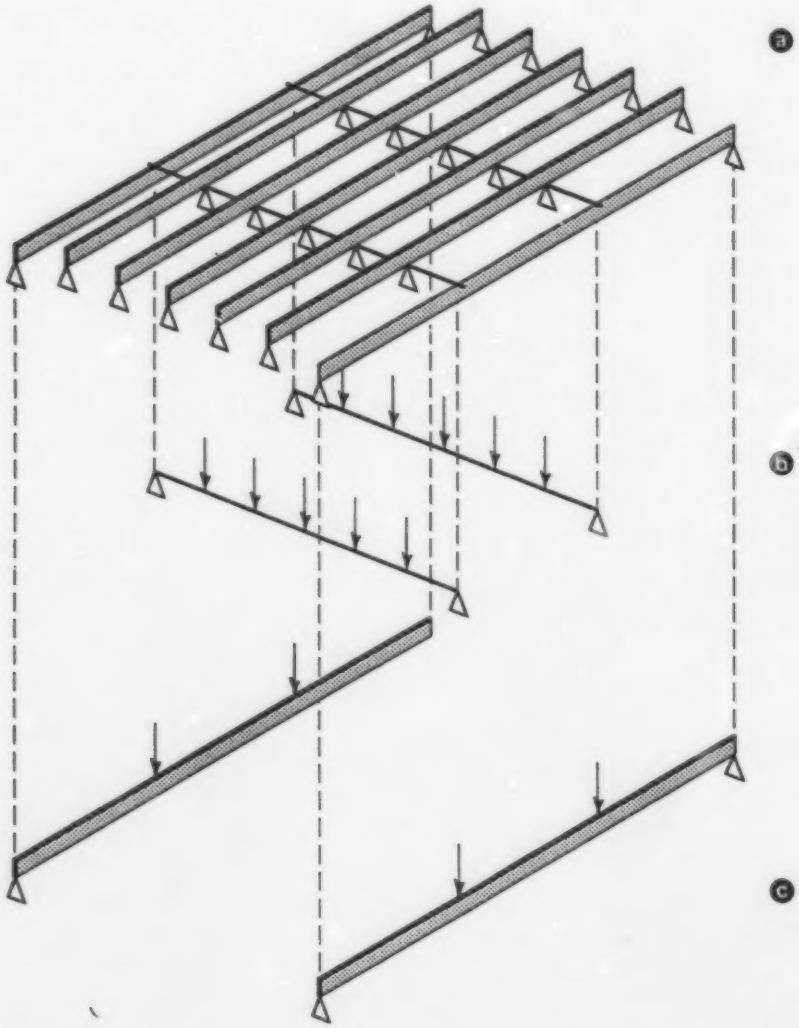

Figure 4.1/ Illustration of the usual practice of determining dead load effects in stringers, floor beams and girders.

4.2/ Rigorous Analysis

In order to assess quantitatively the influence of component interaction on load effects due to dead loads, the Adair bridge was analyzed by the grillage analogy method under a uniformly distributed load. The grillage used in this analysis is shown in Fig. 4.2. As indicated in this figure, several 'dummy' transverse members with negligible stiffnesses were used merely to provide additional nodes to which loads could be applied to simulate uniform distribution.

Bending moments in the middle stringer obtained by grillage analysis are compared in Fig. 4.3 with the corresponding moments obtained by the usual method in which the floor beams are assumed to provide rigid restraint against vertical deflection. Several significant observations can be made regarding this comparison: (a) The flexibility of the girders, hence that of the intermediate supports to stringers, is large enough to eliminate altogether the negative moments from the stringers; (b) the usual simplified method wrongly predicts that the maximum positive moments take place in the external spans of stringer; and most importantly (c) the usual method underestimates, by a large margin, the maximum moments in the stringers.

The relatively large bending moments in the stringers at mid-span, indicate clearly that a part of the total moments at mid-span, which are assigned by the usual method in entirety to the girders, is, in fact, taken by the stringers as well. From the results of grillage analysis it was found that 13% of the total mid-span moments due to dead load directly above the stringers, is taken by stringers themselves, thus relieving the girders of 13% moments.

Similarly, it was found that due to component interaction, the maximum dead load moments in the floor beams are also reduced by about 13%.

The stresses due to factored dead loads, obtained by rigorous analysis, are also listed in Table 4.1 along with the stresses and strains that are available for factored live loads.

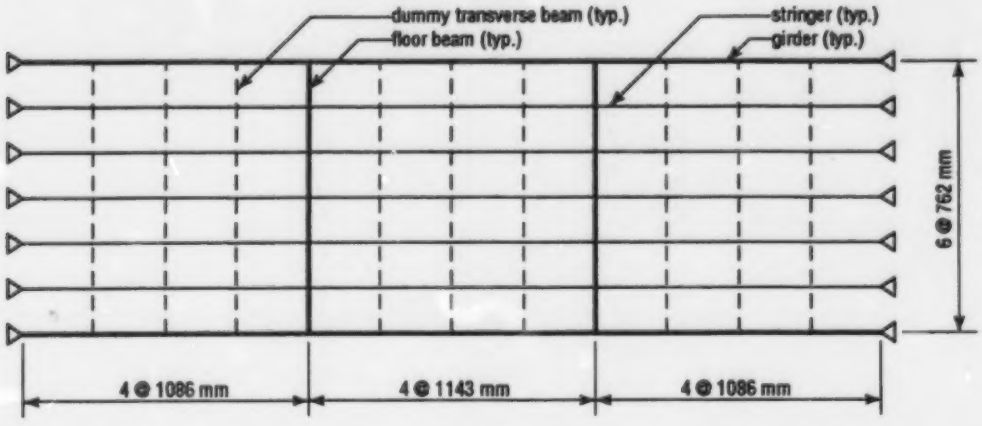

Figure 4.2/ Grillage used for dead load analysis

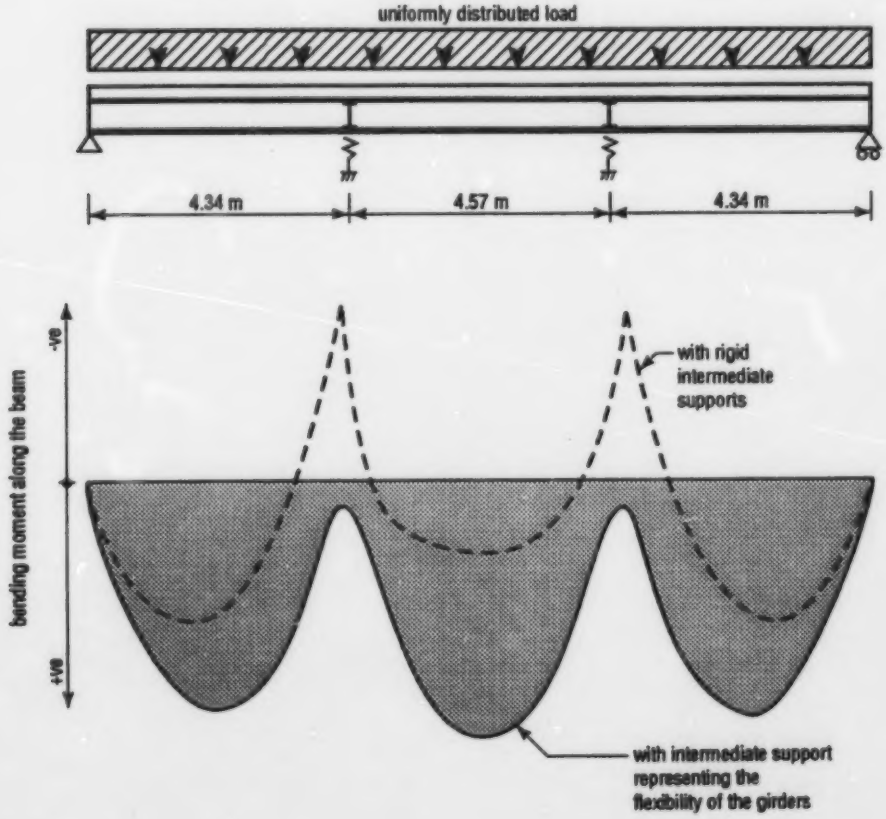

Figure 4.3/ Dead load bending moments in a stringer

5/ Instrumentation and Testing

5.1/ Instrumentation

It was decided to monitor the response of the structure mainly through strain measurements. Accordingly, electrical resistance strain gauges and demountable strain transducers were installed on the various components as described in the following.

5.1.1/ Girders

As shown in Fig. 5.1, both girders were installed with strain measuring devices to record longitudinal strains at the mid-span and at sections close to each support. At each section, strains were measured at three locations, being top and bottom flanges and midway on the web. Girder deflections at the mid-span were measured through deflection transducers.

5.1.2/ Floor Beams

At their mid-spans, the floor beams carry a stringer, because of which it is difficult to instrument a section exactly midway between the girders. As shown in Fig. 5.1, each of two floor beams was installed with three strain measuring devices at a section that is slightly away from the critical midway section. To assess the degree of rotational restraint at its supports, floor beam no. 1 was also similarly instrumented at a section close to each support.

5.1.3/ Stringers

The stringers were decided to be instrumented at Section BB which is shown in Fig. 5.1 and which lies roughly midway between the west abutment and the closer floor beam. Each stringer at this section was installed with a strain transducer at the bottom flange and an electrical resistance strain gauge near the top of the web. As can be seen in Fig. 5.1, the top flanges of the stringer are embedded in the deck slab because of which it was not feasible to install gauges on these flanges.

The identifying numbers for all the instruments are shown in Fig 5.1.

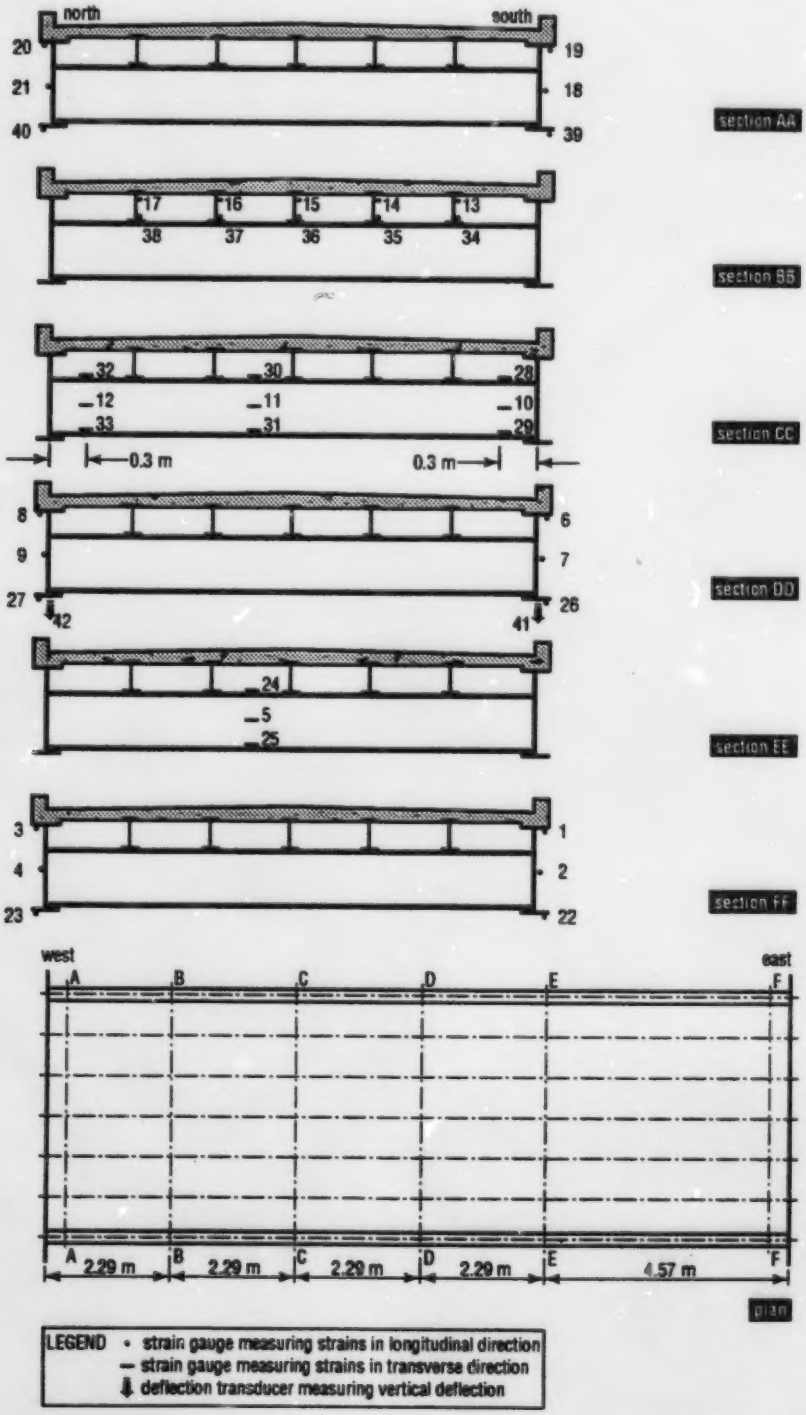

Figure 5.1/ Details of instrumentation

5.2/ Loads

One of two Ministry test vehicles, namely Kenworth, was used for the test. Axle weights corresponding to the three levels of loads employed in the test and axle spacings are given in Table 5.1.

Table 5.1/ Axle weights of the test vehicle

load level no.	no. of concrete blocks	weight in kN for axle no.					total weight, kN
		1	2	3	4	5	
1	12	46	69	69	73	73	330
2	24	48	93	93	105	105	444
3	36	51	116	116	137	137	557

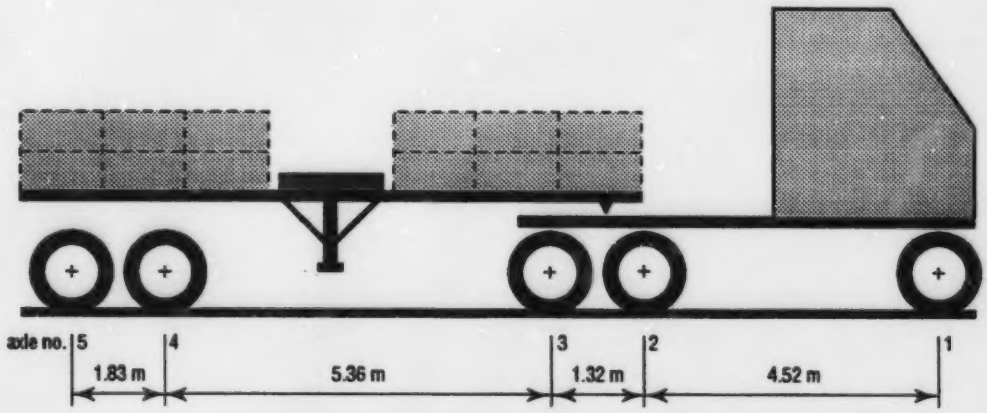

The bridge was tested with the test vehicle in three transverse positions identified in Fig. 5.2. In one of these transverse positions, the vehicle was placed centrally; the other positions being the mirror images of each other, represented as eccentric a position as possible. As can be seen in the photograph in Fig. 5.3, the test vehicle in the eccentric position is very close to the railings of the bridge. It is unlikely that an actual heavy vehicle travelling at normal speed can get so close to the bridge railings.

For each transverse position, the test vehicle was stopped at nine different longitudinal positions. These positions, which were established to induce maximum load effects in different components, are shown in Fig. 5.4.

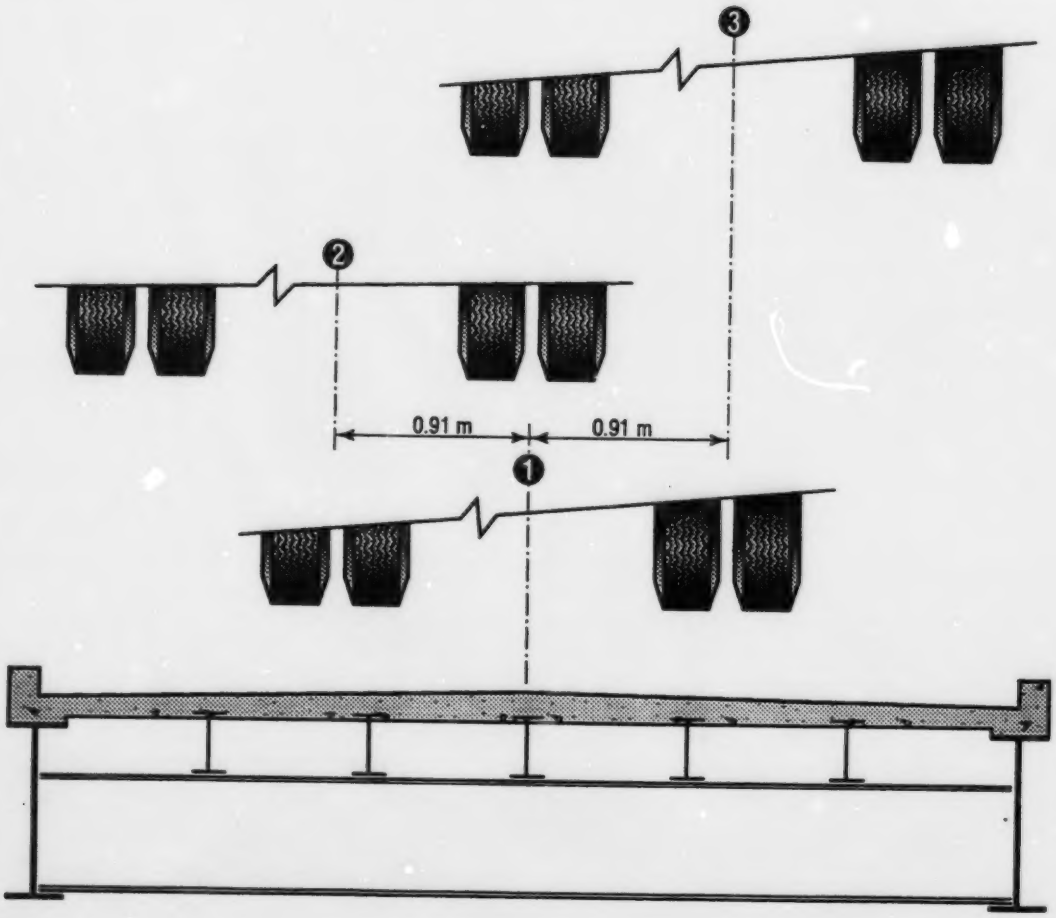

Figure 5.2/ Transverse positions of the test vehicle

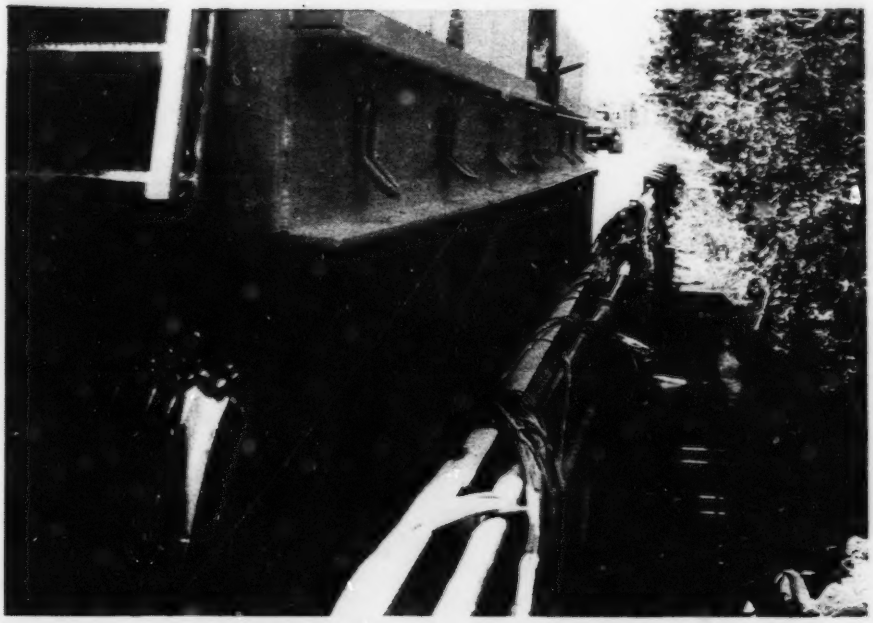

Figure 5.3/ Photograph showing the test vehicle in eccentric position

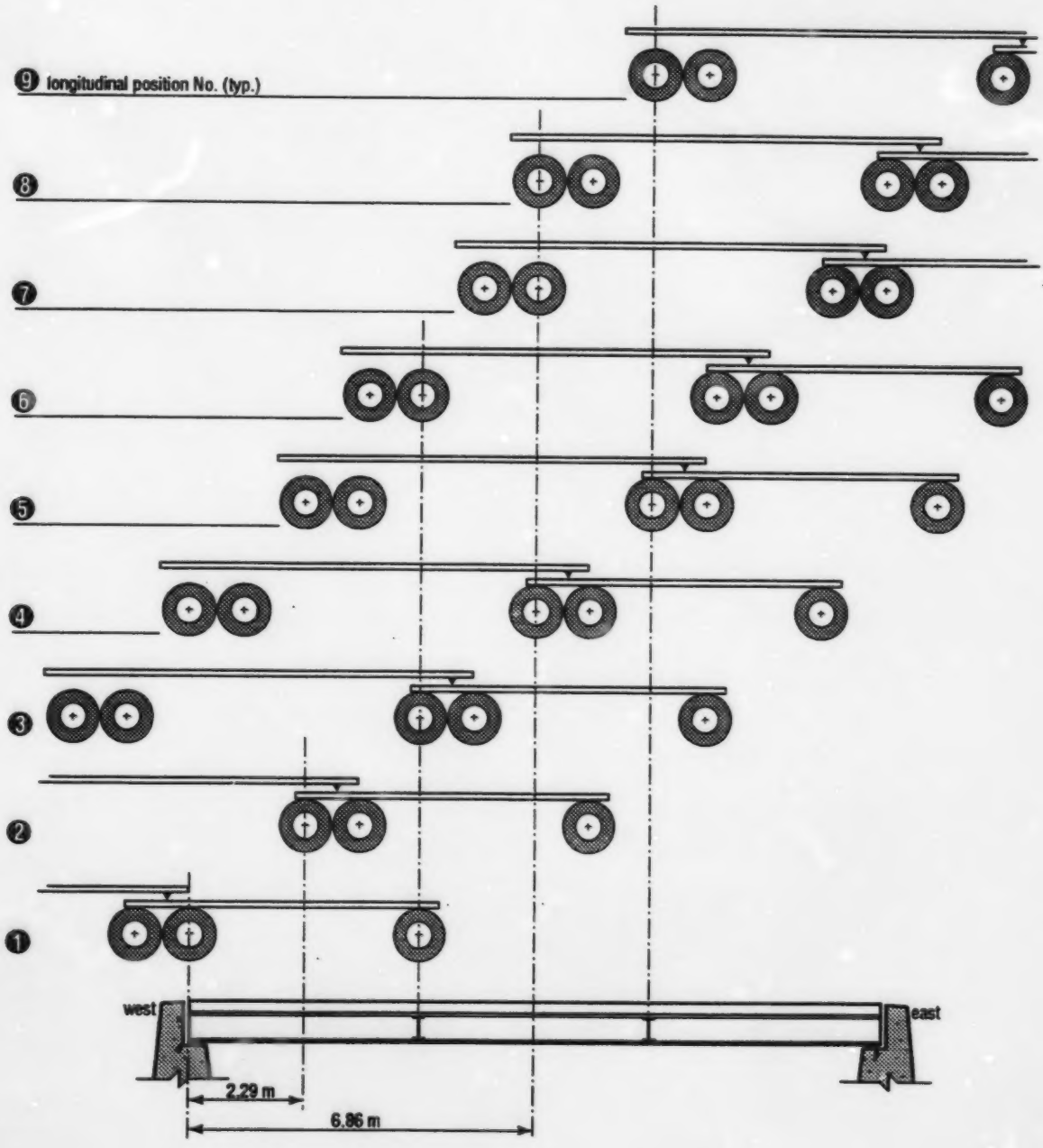

Figure 5.4/ Longitudinal positions of the test vehicle

6/ Recorded Data and Its Interpretation

6.1/ Girders

Mid-span longitudinal strains in the top flange of the north girder are plotted for three different load levels in Fig. 6.1 against the longitudinal positions of the test vehicle. The similarity of patterns for the three load levels, confirms that the instruments were functioning satisfactorily.

Figure 6.1 shows that the maximum strains are induced when the test vehicle is very close to longitudinal position no. 6, it being noted that the strains due to the vehicle in this position, are about 2% smaller than the maximum strains. For the excercise at hand, however, the strains in girders due to the test vehicle in longitudinal position no. 6, are treated as maximum; these strains are listed in Table 6.1, corresponding to the vehicle at three load levels and in different transverse positions.

An asterisk in Table 6.1 and others identifies unreliable readings from an instrument which either stopped functioning or encountered relatively large drift. It is recalled that the difference between the readings taken before and after the placing of test loads on the bridge, is referred to as the "drift."

Girder deflections at the mid-span are recorded in Table 6.2. It is noted, however, that many of these deflections are not reliable because of large drifts observed in the deflection transducers.

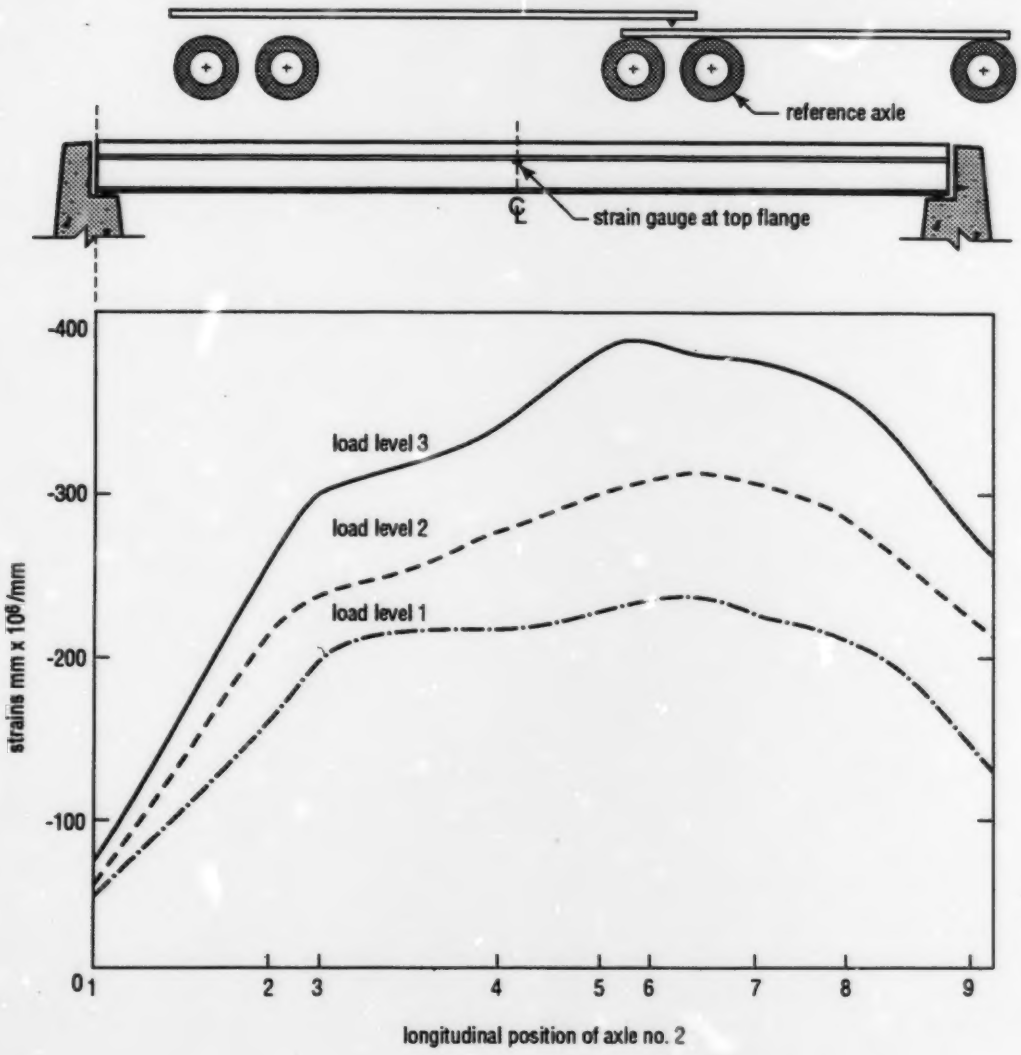

Figure 6.1/ Top flange strains in north girder due to test vehicle in transverse position no.1

Table 6.1/ Strains in girders due to the test vehicle in longitudinal position no. 6

Transverse position no.	north/ south girder	load level no.	strains near west support, mm x 10^6/mm			strains at mid-span, mm x 10^6/mm			strains near east support, mm x 10^6/mm		
			top	mid.	bottom	top	mid.	bottom	top	mid.	bottom
1	N	1	*	-23	-10	-233	-26	179	*	*	*
		2	52	-14	-16	-308	-40	243	-6	-40	-57
		3	40	-20	-30	-380	-49	297	34	46	-67
	S	1	49	23	8	-201	-23	*	0	-26	*
		2	46	-14	*	-273	-29	232	29	-34	*
		3	-20	60	-152	-385	-40	317	34	-46	*
2	N	1	*	-29	-20	-288	-43	225	-3	43	-76
		2	*	-29	-43	-383	-52	308	29	-58	-116
		3	17	-83	*	-512	-69	*	*	-83	-144
	S	1	-17	17	*	-135	-12	113	12	15	*
		2	-9	23	-37	-181	-14	141	-26	-12	*
		3	-17	*	-93	-242	-23	*	17	-32	*
3	N	1	-29	-12	-17	-149	-17	112	-17	-20	-17
		2	72	29	*	-210	-29	154	17	-83	*
	S	1	-23	40	*	-262	*	234	20	-43	*
		2	-32	58	*	-371	-43	317	32	-60	*

Table 6.2/ Girder deflections at mid-span due to the test vehicle in longitudinal position no. 6

transverse position no.	load level no.	deflections in mm	
		north girder	south girder
1	1	10.0	9.9
	2	13.2	11.6
	3	15.0	15.7
2	1	14.8	5.6
	2	19.0	7.0
	3	20.8	7.0
3	1	6.9	12.1
	2	8.4	17.2

6.1.1/ Symmetry of Data

Because of the symmetry of the structure and load cases, strains in girders have their mirror image counterparts; these corresponding strains are used to confirm the validity of the measured data. Some examples of pairs of corresponding strains are given in Table 6.3, in which it can be observed that the corresponding strains, while not being exactly the same, are fairly close to each other, thus again confirming the validity of the measured data.

6.1.2/ Linearity

Since the total weight was increased nearly proportionally on axles 2 through 5, the weight on these axles can be regarded as a fair measure of the bending moments in the girders. Accordingly, certain strains in the girders are plotted in Fig 6.2, against the total weight of these four axles. It can be seen in this table that girders have a tendency to "soften" slightly at higher load levels. This effect may be attributed to the loss of bearing restraint which depends almost entirely on friction between the girder and the abutment.

Despite the slightly non-linear load-strain relationship, all the strains were recovered upon the removal of the loads indicating elastic response and confirming that the bridge can sustain similar loads at any time.

Table 6.3/ Symmetry check for girders due to the test vehicle in longitudinal position no. 6

load level	transverse pos. no.	gauge no.	strain mm x 10^6/mm		gauge no.	transverse pos. no.
			north girder	south girder		
2	1	27	243	233	26	1
3	1	27	297	317	26	1
1	1	8	-233	-201	6	1
2	1	8	-308	-273	6	1
3	1	8	-380	-385	6	1
1	2	27	225	234	26	3
2	2	27	308	317	26	3
1	2	8	-288	-262	6	1
2	2	8	-383	-371	6	1

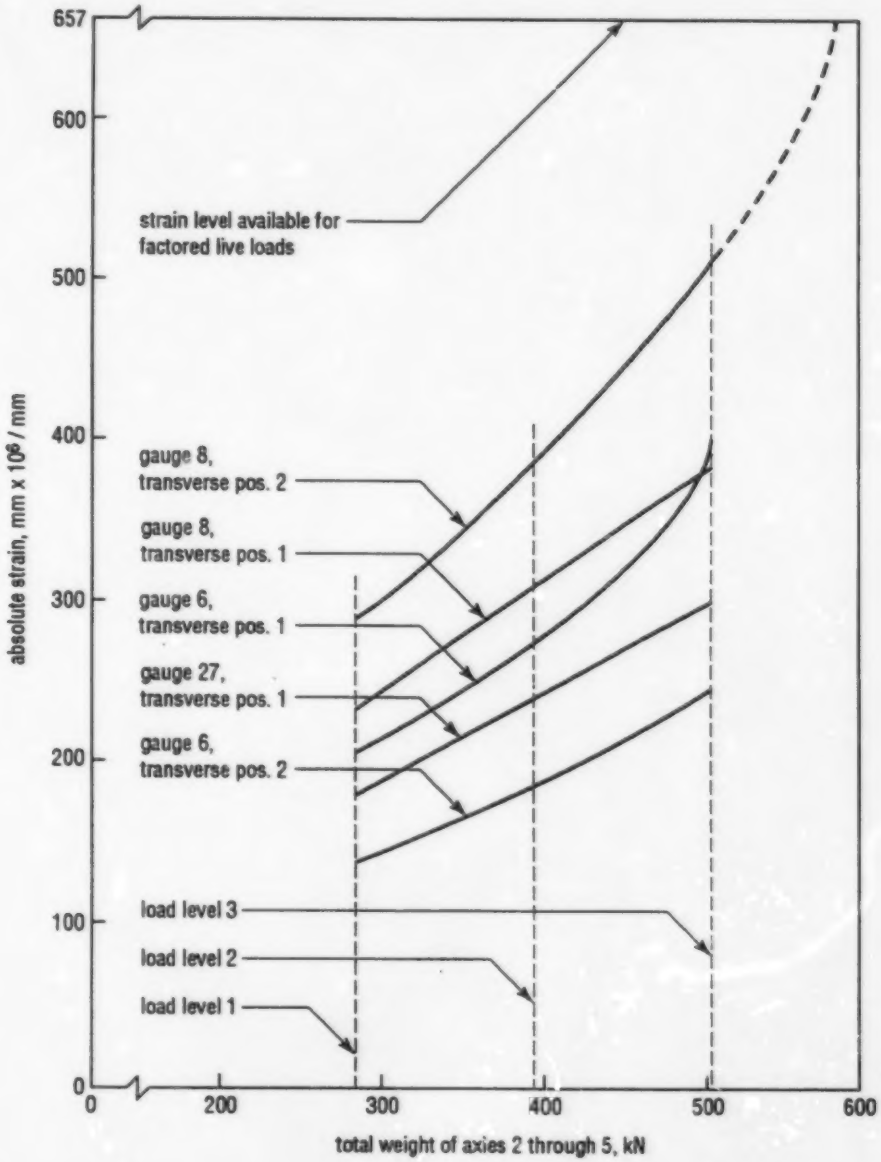

Figure 6.2/ Load-strain relationships for girders due to the test vehicle in longitudinal position no. 6

6.1.3/ Bearing Restraint

Mid-span strains in the top and bottom flanges of the two girders due to two load cases, are plotted in Fig. 6.3 against the longitudinal position of the test vehicle. It can be seen in this figure and also in Table 6.1, that the strains in the top flanges are always much larger in magnitude than those in the bottom flange. This observation confirms the presence of fairly large compressive strains at the bottom flanges near supports. Large compressive strains in bottom flanges near the supports, were also recorded by the strain transducers attached at these locations.

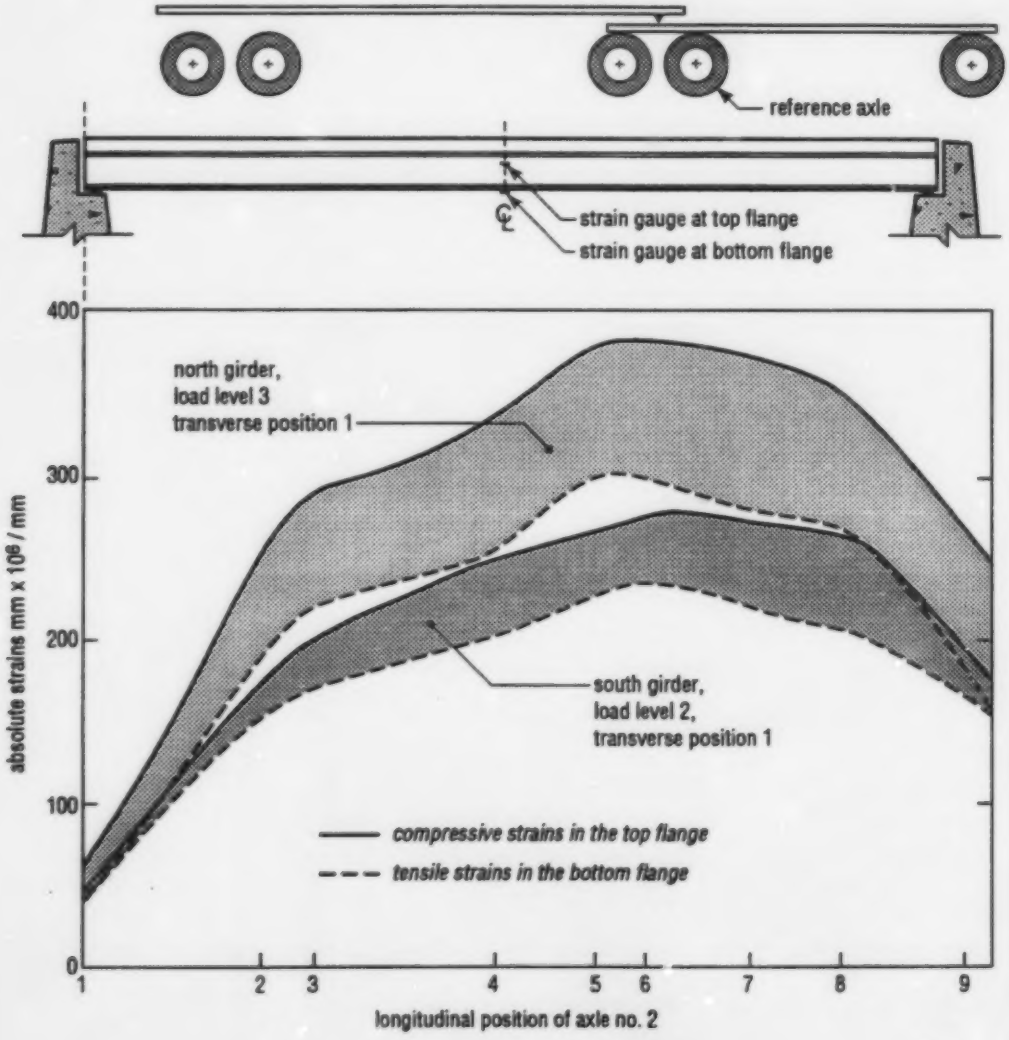

Figure 6.3/ Girder strains at mid span

Larger magnitudes of strains in the top flanges, also indicate that the degree of composite action between the deck slab and the girders, is rather limited. Because of this limited composite action, the top flange stresses, getting little help from the bearing restraint, govern the load carrying capacity of the girders.

It is important to note that, unlike the case in usual slab-on-girder bridges, the bearing restraint does not provide the extra reserve of strength in the bridge under consideration.

6.1.4/ Calculated Strains

Several uncertainties come in the way of predicting the stresses and strains in the girders due to the test loads. One such uncertainty relates to the effective span of the girders. As can be seen in Fig. 2.1, a 0.46 m length of the girder rests on the concrete abutment. Because of this rather large bearing length compared to the span, relatively large errors are involved in ascertaining the position of the centre of gravity of the support reaction, which can be taken as the location of the idealized point support for the girder.

Another difficulty concerning the prediction of strains due to test loads, relates to the absence of mechanical shear connection between the girders and the concrete deck slab, because of which the degree of composite action between the two components becomes uncertain. The bearing restraint that may exist at the interface of the bottom flange of the girders and the concrete abutment, poses yet another uncertainty.

For purposes of preliminary calculation, it was assumed that (a) the point support for the girders, lies midway in the bearing length; (b) there is no composite action between the deck slab and girder; (c) the girders are truly simply-supported, i.e. the bearing restraint force is zero; and (d) the girders sustained all the applied loading. On the basis of these assumptions, it was found that for the most eccentric transverse position, the test vehicle would induce maximum girder stresses, both tensile and compressive, of 81, 111 and 142 MPa corresponding to load levels 1, 2 and 3, respectively; these stress levels corrsepond to strains of 392, 538, and 689 x 10^{-6} mm/mm, respectively in the steel components.

6.1.5/ Interpretation of Measured Strains

The maximum observed strains, as discussed in detail earlier, were compressive strains shown as negative herein. These strains corresponding to the eccentric load cases were found to be -288, -383 and - 512 x 10^{-6} mm/mm. Due to the test vehicle at load level 1, 2 and 3, respectively. The observed maximum strains in the top flanges are about 25% smaller than the respective calculated strains. This reduction could be partly due to the effective span being smaller than assumed in the calculations,

partly due to some composite action between the girders and the slab and partly due to the stringers sustaining a portion of the applied loading as discussed in Sec. 4.2.

Since the induced maximum strains were much smaller than the available strains for live loads, the proof load corresponding to level 3 loading can be regarded as a very conservative estimate of the load carrying capacity of the girders. A more realistic, and still safe-side, estimate of the strength of the girders, can be obtained by extrapolating the non-linear strain curve to 657 x 10^{-6} mm/mm; this, as indicated in Table 4.1, is the available strain for live loads. The strain capacity that is available in the girders can sustain safely a total load of about 580 kN; this extrapolated proof load shown in Fig. 6.2, is about 15% larger than the actual proof load.

6.2/ Floor Beams

It can be shown readily that the maximum moment in a floor beam of the Adair bridge is caused when the test vehicle is place transversely between either transverse positions 1 and 2 or between 1 and 3. It can also be shown that the moments at the instrumented section near the mid-span of the floor beam due to the vehicle in transverse position 1, are about 6% smaller than the maximum moments. To obtain maximum strains, therefore, one must multiply the observed strains due to the test vehicle in transverse position 1, by a factor of 1.06.

The strains in floor beam no. 1 near its mid-span for some cases, are plotted in Fig. 6.4 against the longitudinal positon of the test vehicle. As can be seen in this figure, the strain curve has two distinct peaks, the first one corresponding to the front tandem of the test vehicle and the second to the rear. The second tandem induces maximum strains at longitudinal position no. 6.

Similar strain plots for floor beam no. 2 drawn in Fig. 6.5 indicate that for this floor beam, the maximum load effects are induced at longitudinal position no. 9.

Strains in floor beam nos. 1 and 2 due to the test vehicle in longitudinal positions nos. 6 and 9, respectively, are tabulated in Table 6.4.

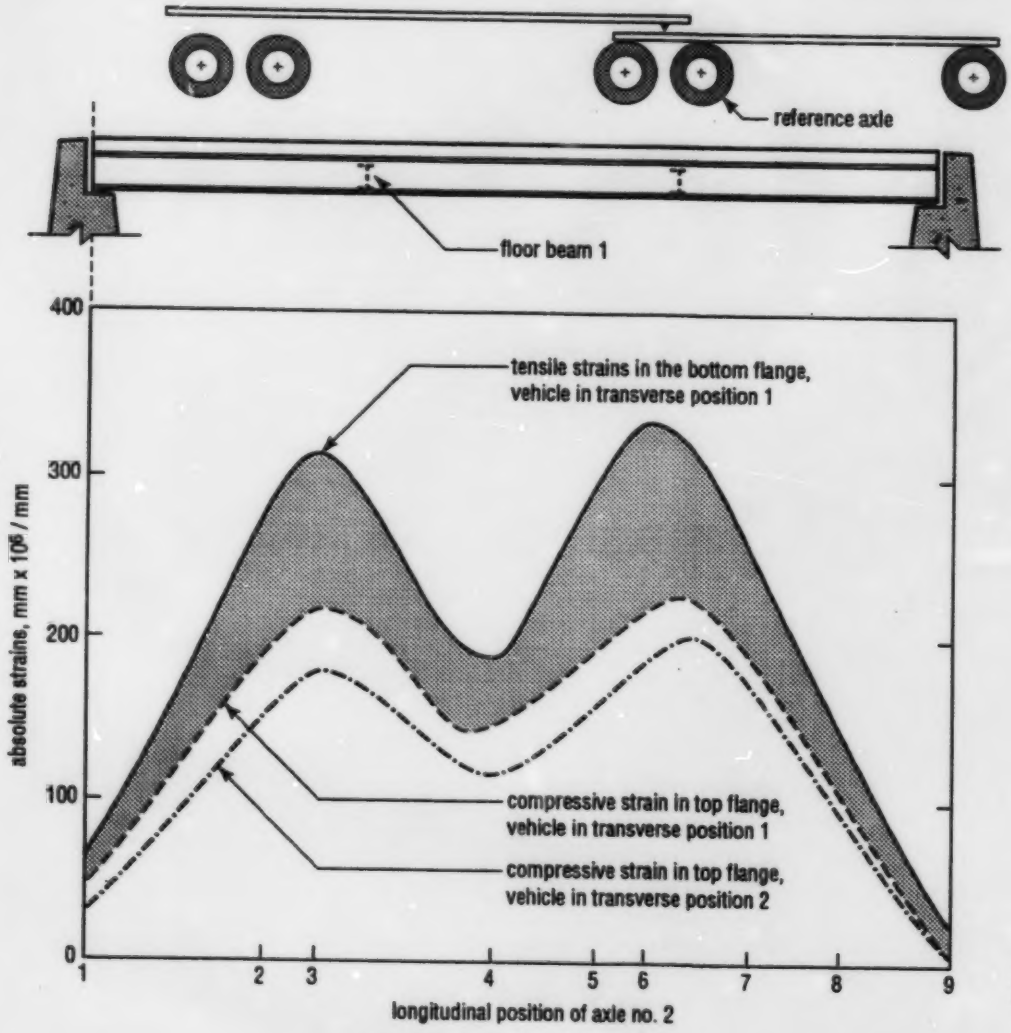

Figure 6.4/ Strains near the mid-span of floor beam 1 due to test vehicle at load level 3

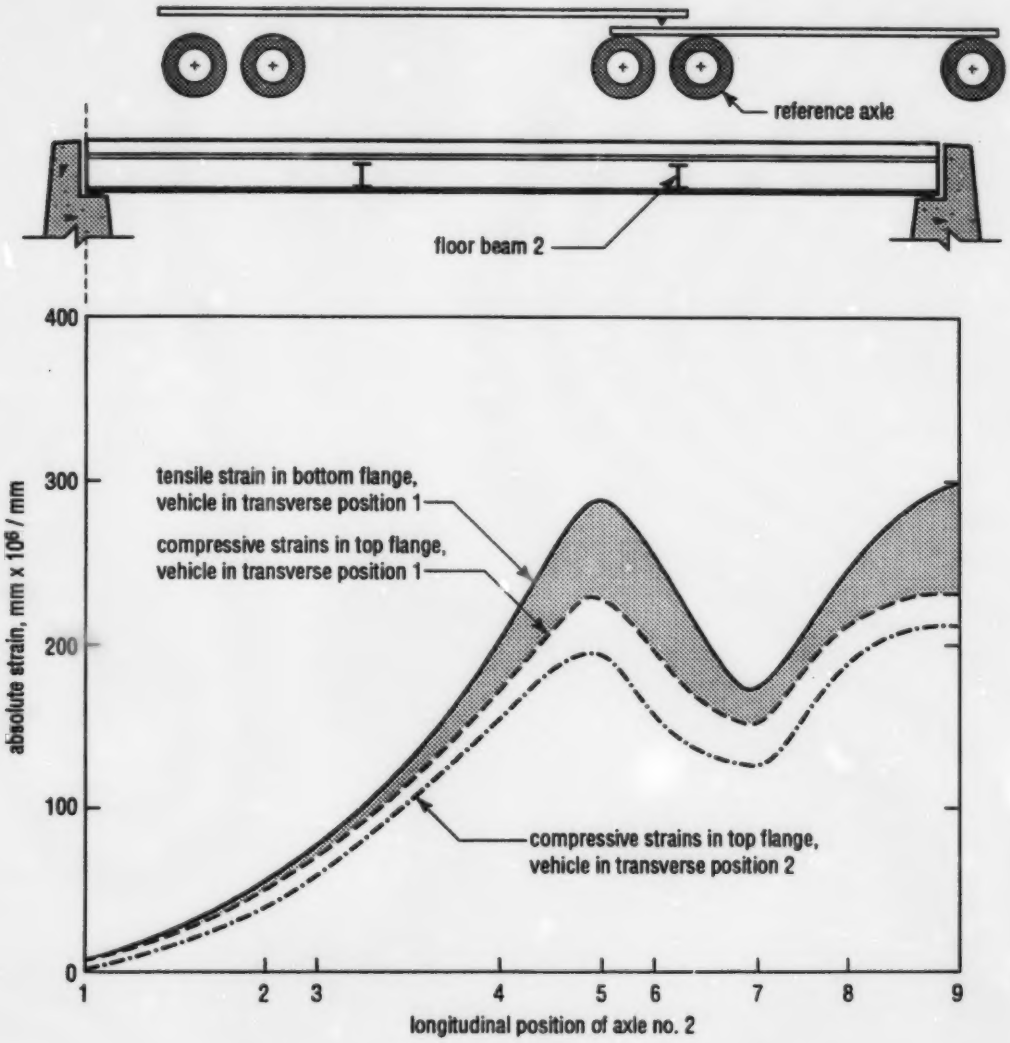

Figure 6.5/ Strains near the mid-span of floor beam 2 due to test vehicle at load level 3

Table 6.4/ Strains in floor beams

floor beam no.	transverse position no.	load level no.	strains near north girder mm x 10^6/mm			strains near mid span, mm x 10^6/mm			strains near south girder mm x 10^6/mm		
			top	mid.	bottom	top	mid.	bottom	top	mid.	bottom
1 (vehicle in longitudinal position 6)	1	1	-36	9	32	-125	*	185	*	9	29
		2	-50	9	54	-176	*	254	*	9	50
		3	-57	14	72	-216	*	330	*	9	75
	2	1	-41	3	36	-104	*	156	*	9	13
		2	-55	9	56	-140	*	215	*	3	31
		3	-85	14	82	-181	*	284	*	3	42
	3	1	-20	6	22	-88	*	134	*	9	33
		2	-27	6	28	-124	*	190	*	6	50
2 (vehicle in longitudinal position 9)	1	1				-124	3	153			
		2				-182	17	236			
		3				-226	-14	300			
	2	1				-118	-6	153			
		2				-166	6	222			
		3				-213	3	279			

6.2.1/ End Restraint

It can be seen in Table 6.4 that near the support at girders, the strains at top and bottom flanges of the floor beams are of similar orders of magnitude. These strains are consistent with bending moments that are expected at the instrumented sections in a simply-supported beam. Thus it was confirmed that the floor beams are simply-supported with the girders offering little rotational restraint.

6.2.2/ Linearity

Strains in floor beams are plotted in Fig. 6.6 against the weights of the rear or front tandems of the test vehicle. It can be seen in this figure that load-strain relationships are perfectly linear. Since all the strains induced by live loads were recovered completely upon the removal of the test vehicle, the behaviour of the floor beams is confirmed to be linear-elastic up to the proof load level.

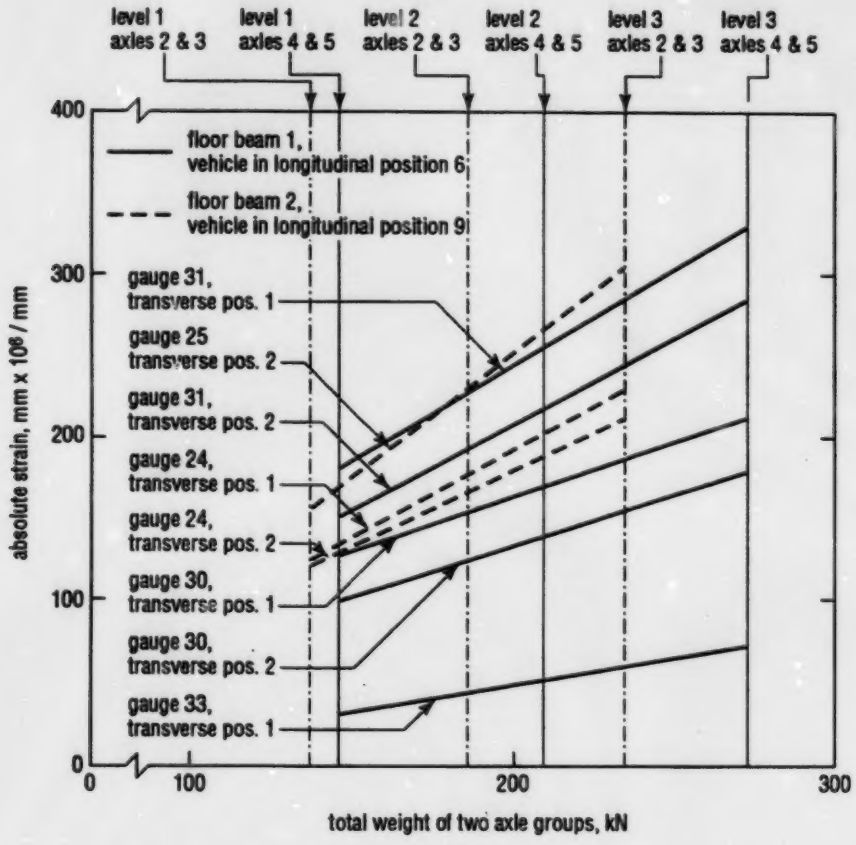
level 1 axles 2 & 3
level 1 axles 4 & 5
level 2 axles 2 & 3
level 2 axles 4 & 5
level 3 axles 2 & 3
level 3 axles 4 & 5
floor beam 1, vehicle in longitudinal position 6
floor beam 2, vehicle in longitudinal position 9
gauge 31, transverse pos. 1
gauge 25 transverse pos. 2
gauge 31, transverse pos. 2
gauge 24, transverse pos. 1
gauge 24, transverse pos. 2
gauge 30, transverse pos. 1
gauge 30, transverse pos. 2
gauge 33, transverse pos. 1
absolute strain, mm x 10⁶ / mm
total weight of two axle groups, kN
0
100
200
300
400

Figure 6.6/ Load-strain relationships for floor beams

6.2.3/ Differences Between Top and Bottom Strains

Floor beam strains near the girders have confirmed that the floor beams have practically no lateral restraint at their supports. The differences between the top and bottom strains, that can be seen in Figs. 6.4 and 6.5 and Table 6.4, can not, therefore, be due to bearing restraint. It seems that the deck slab in conjunction with the relatively short lengths of the stringer webs, provides some composite action to the floor beams.

6.2.4/ Maximum Strains

A simplified analysis presented by Bakht and Jaegar (1985) shows readily that for the structure under consideration, a floor beam sustains about 83% of the weight placed on it directly. If it is assumed that

the rear tandem of the test vehicle is placed directly over the floor beam, then the strain corresponding to the maximum moment induced in the floor beam is found to be 450 x 10^{-6} mm/mm.

The maximum observed strain available in a floor beam, noted in Table 6.4, is 330 x 10^{-6} mm/mm. By multiplying this strain with the factor 1.06 discussed earlier, one gets the maximum extrapolated strain of 350 x 10^{-6} mm/mm. The fact that this strain is smaller than the calculated maximum strain 450 x 10^{-6} mm/mm, clearly indicates the presence of some composite action in the middle region of the floor beam.

As noted in Table 4.1, the strain available in the floor beams for factored live loads is 851 x 10^{-6} mm/mm. Since this strain is considerably smaller than the observed maximum, level 3 test load can be regarded as a very conservative estimate of the capacity of the floor beams. By extrapolation, however, one can conclude that the actual capacity of the floor beam is more than double that indicated by this proof load. The extrapolated proof load = 626 kN.

6.3/ Stringers

Strains in bottom flanges of some stringers are plotted in Fig. 6.7 against the longitudinal position of the test vehicle. As for floor beams, the strain curves for stringers also have two peaks, with the peak near longitudinal position no. 2 representing the highest strains. From extrapolation of the curves given in Fig. 6.7, it is concluded that the maximum strains induced in the bottom flanges of the stringers due to test vehicles in longitudinal position no. 2 are, at most, 10% smaller than the maximum strains. To be on the safe side, the values of observed strains corresponding to longitudinal position 2 will be multiplied by 1.10 to obtain the maximum strains.

Stringer strains corresponding to longitudinal position no. 2, are given in Table 6.5. It can be seen in this table that for all cases, the strains near the top flanges are very small in magnitude compared to the bottom flanges. This observation shows clearly that despite the absence of mechanical shear connecting devices, the stringers act compositely with the slab even at the maximum applied loads.

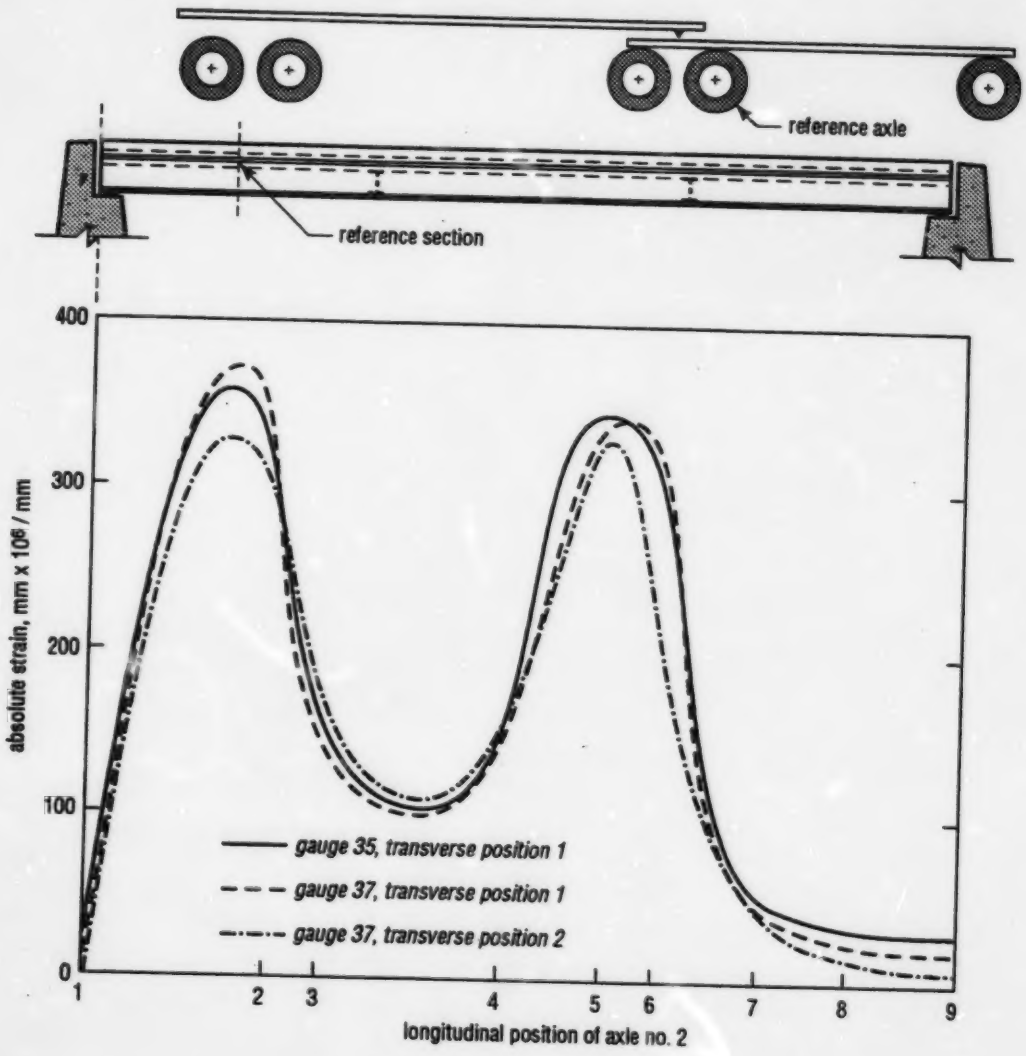

Figure 6.7/ Bottom flange strains in stringers due to test vehicle at load level 2

Table 6.5/ Strains in stringers due to the test vehicle in longitudinal position no. 2

transverse position no.	load level	strains in stringer no. 1, mm x 10^6/mm		strains in stringer no. 2, mm x 10^6/mm		strains in stringer no. 3, mm x 10^6/mm		strains in stringer no. 4, mm x 10^6/mm		strains in stringer no. 5, mm x 10^6/mm	
		top	bottom	top	bottom	top	bottom	top	bottom	top	bottom
1	1	0	111	17	220	-6	184	0	212	9	120
	2	3	50	3	299	3	226	3	272	17	152
	3	6	183	6	363	0	270	-6	341	40	202
2	1	-6	151	0	209	-3	179	-3	156	3	74
	2	6	192	6	250	-3	219	-6	192	6	94
	3	-6	245	-12	311	-12	262	-9	242	9	132
3	1	-9	73	-9	156	3	177	9	200	15	132
	2	-9	92	-6	176	-17	168	-17	227	3	150

The maximum recorded strain of 363 x 10^{-6} mm/mm, multiplied by the factor 1.10 discussed above, gives the actual maximum strains of 399 x 10^{-6} mm/mm. This strain level is considerably below the strain level of 754 x 10^{-6} mm/mm which, as shown in Table 4.1, is available for factored live loads. In spite of this observation, the maximum test load, and not the extrapolated load based on available strains, will be taken as a measure of the load carrying capacity of the stringers. This highly conservative approach is being adopted in light of observations that in the absence of mechanical shear connection, the composite action between the slab and the steel beam breaks down completely at higher load levels (Bakht, 1988).

As can be seen Fig. 6.8, the load-strain curves for bottom flanges of the stringers, are exactly, or very nearly, linear. All these strains were also recovered completely upon the removal of test loads. These observations confirm that the test loads can be regarded as proof loads for the stringers.

Strains in the bottom flanges of all stringers at the instrumented section are plotted in Fig. 6.9 for three transverse positions of the test vehicle at load level 2 and in longitudinal position 5. The symmetry of the observed transverse distribution of longitudinal strains not only confirms the validity of the measured data, but also shows that all stringers have similar degrees of composite action with the deck slab.

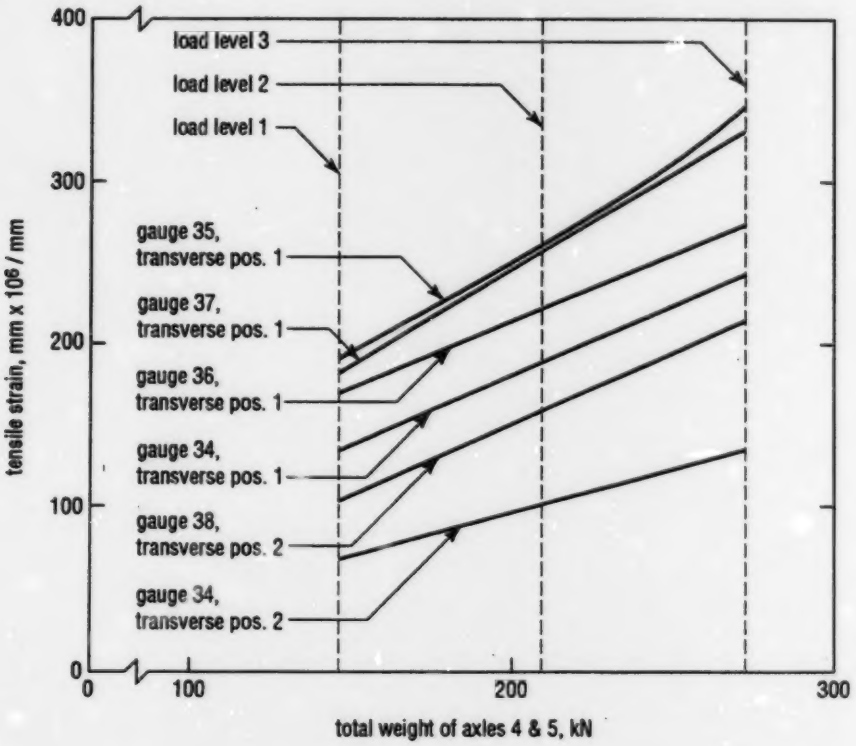

Figure 6.8/ Load-strain relationships for stringers due to the test vehicle in longitudinal position no. 5

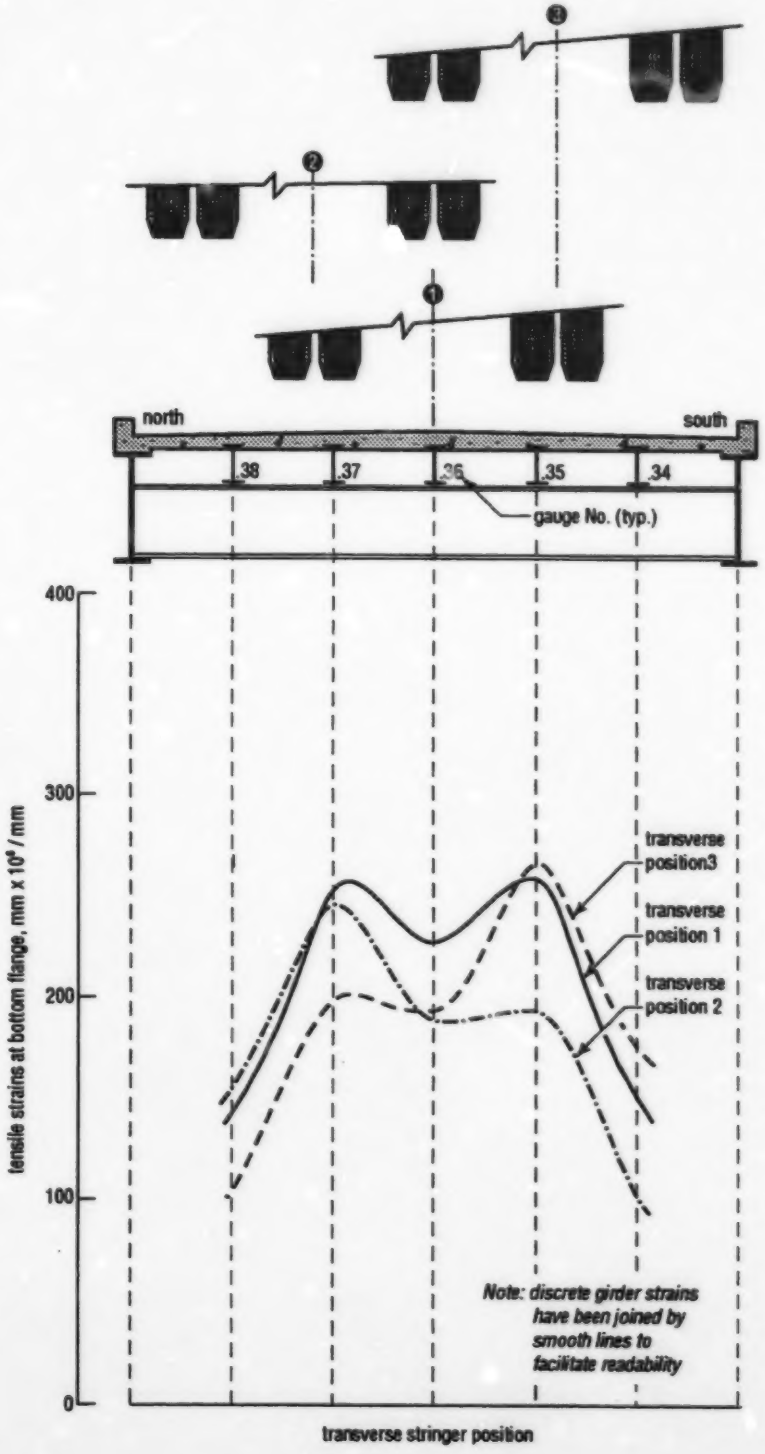

Figure 6.9/ Transverse distribution of bottom flange strains in stringers due to test vehicle at load level 2 and longitudinal position 5

7/ Strength Evaluation

7.1/ Proof Loads

From discussion in Chap. 6, it is summarized that the proof loads corresponding to different components of the bridge, are as shown in Table 7.1. This table also identifies the axle nos. which constitute the proof load for different components.

Table 7.1/ Proof loads for different components

component	axle nos. of test vehicle constituting the proof load	actual proof load, kN	extrapolated proof load, kN
girder	2 through 5	506	580
floor beam	4 and 5	274	626
stringer	4 and 5	274	274

7.2/ Equivalent Loads

As discussed by Mufti and Bakht (1991), equivalence between the various configurations of the test vehicle and the OHBDC Evaluation loads can be established with the help of the Equivalent Base Length Concept. Equivalent Base Length for the various sub-configurations of the OHBDC Evaluation load and stet relevant subconfigurations of the test vehicle are shown in Fig. 7.1. As shown in this figure, axles 4 and 5 are equivalent to the OHBDC Evaluation load when they carry a load of about 292 kN. Similarly, axles 2 through 5 are equivalent to the OHBDC Evaluation load when they carry 462 kN in the same proportion as the axle loads at load level 3.

7.3/ Scale-down Factors

The OHBDC (1983) defines through Clause 14 - 7.2.1 a non-dimensional quantity F which is called the scale-down factor and is given by

$$F = \frac{\phi R_n - \text{Load effects due to factored dead loads}}{\text{Load effects due to factored live loads}}$$

The numerator in the above equation represents the strength of the bridge that is available for live loads. For evaluation by proof testing, it can be demonstrated that the proof load reduced appropriately to account for the dynamic load allowance, represents a conservative estimate of the

strength of the bridge that is available for live loads. In this case, the denominator of the above equation should accordingly be considered as the equivalent Evaluation load corresponding to the various subconfigurations of the test load, as discussed in Sec. 7.1, multiplied by the live load factor.

The dynamic load allowance, I, for bridges with spans less than 22 m is 0.30, and the live load factor is 1.25 if the bridge is to be re-evaluated in five years.

Accounting for I = 0.30 and the live load factor of 1.25, the static proof loads on the various components of the bridge are as given in Table 7.2, along with the resulting scale-down factors. As shown in this table, the scale-down factors corresponding to actual proof loads are 0.67, 0.62 and 0.62 for girders, floor beams and stringers, respectively; by using extrapolated proof loads, these factors can be upgraded to 0.76, 1.42 and 0.62, respectively.

Table 7.2/ Scale-down factors

component	axle nos. of test vehicle constituting proof load	equivalent evaluation load, kN	actual proof load, kN	proof load discounted for I and load factor, kN	scale-down factor, F
Girder	2 through 5	462	506	311	0.67
Floor Beam	4 and 5	292	274	169	0.62
Stringer	4 and 5	292	274	169	0.62

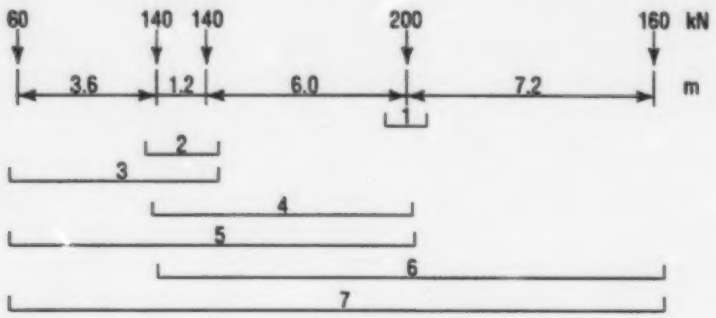

The OHBDC Design Truck and its Subconfigurations

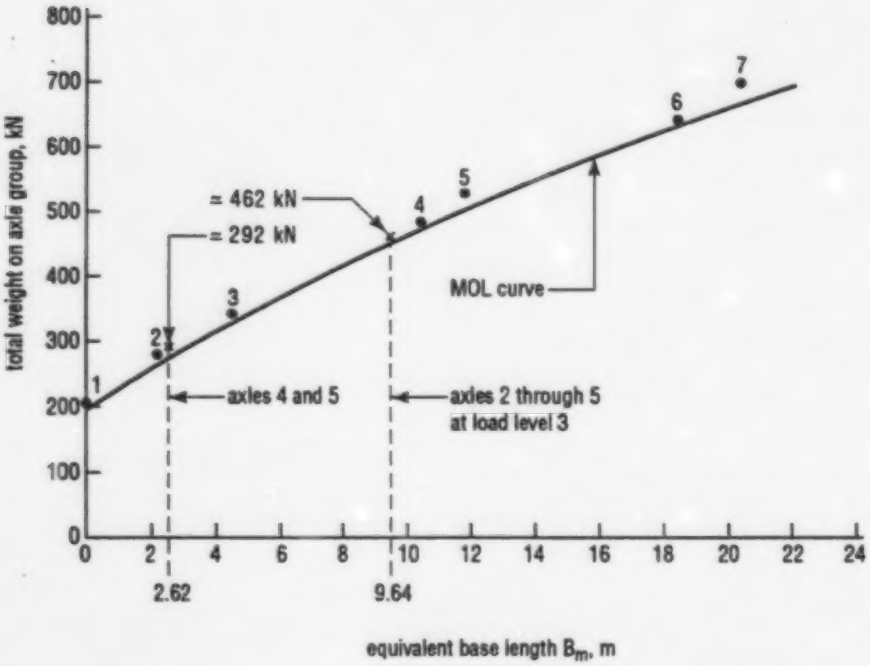

Figure 7.1/ Total axle weights plotted against equivalent base length

7.4/ Posting Loads

For F = 0.67, the charts given in Figs. 6.5 - 7.3(a), (b) and (c) of the OHBDC (1983), give for girders, posting loads of 15, 20 and 29 tonnes respectively for level 1, 2 and 3 evaluation loads. For floor beams and stringers, F = 0.62 leads to posting loads of 12, 19 and 26 tonnes. Extrapolation of test loads, does not present any advantage since stringers, whose extrapolated proof load is the same as the actual proof load, govern the posting loads.

8/ Recommendation

Based on a careful analysis of the test data, it is recommended that the posting on the bridge be upgraded either to a single posting of 12 tonnes, or to a triple posting of 12, 19 and 26 tonnes.

References

[1] Bakht, B. and Jaeger, L.G. "Bridge Analysis Simplified." McGraw Hill, 1985.

[2] Bakht, B. "Ultimate Load Test of a Slab-on-girder Bridge." Research Report SRR-88-03. Ministry of Transportation of Ontario, 1988.

[3] Mufti, A. A. and Bakht, B. "Strength Evaluation of an old T-Beam Bridge." Research Report SRR-91-06. Ministry of Transportation of Ontario, 1991.

[4] "Ontario Highway Bridge Design Code." Second Edition. Ministry of Transportation of Ontario, 1983.